

Review

# Mott-Anderson Transition in Molecular Conductors: Influence of Randomness on Strongly Correlated Electrons in the $\kappa$ -(BEDT-TTF)<sub>2</sub>X System

Takahiko Sasaki <sup>1,2</sup>

<sup>1</sup> Institute for Materials Research, Tohoku University, Katahira 2-1-1, Aoba-ku, Sendai 980-8577, Japan; E-Mail: takahiko@imr.tohoku.ac.jp; Tel.: +81-22-215-2025; Fax: +81-22-215-2026

<sup>2</sup> JST-CREST, Tokyo 102-0076, Japan

Received: 12 March 2012; in revised form: 18 April 2012 / Accepted: 20 April 2012 /

Published: 8 May 2012

---

**Abstract:** The Mott-Anderson transition has been known as a metal-insulator (MI) transition due to both strong electron-electron interaction and randomness of the electrons. For example, the MI transition in doped semiconductors and transition metal oxides has been investigated up to now as a typical example of the Mott-Anderson transition for changing electron correlations by carrier number control in concurrence with inevitable randomness. On the other hand, molecular conductors have been known as typical strongly correlated electron systems with bandwidth controlled Mott transition. In this paper, we demonstrate our recent studies on the randomness effect of the strongly correlated electrons of the BEDT-TTF molecule based organic conductors. X-ray irradiation on the crystals introduces molecular defects in the insulating anion layer, which cause random potential modulation of the correlated electrons in the conductive BEDT-TTF layer. In combination with hydrostatic pressure, we are able to control the parameters for randomness and correlations for electrons approaching the Mott-Anderson transition.

**Keywords:** organic conductor; Mott transition; Anderson localization; X-ray irradiation

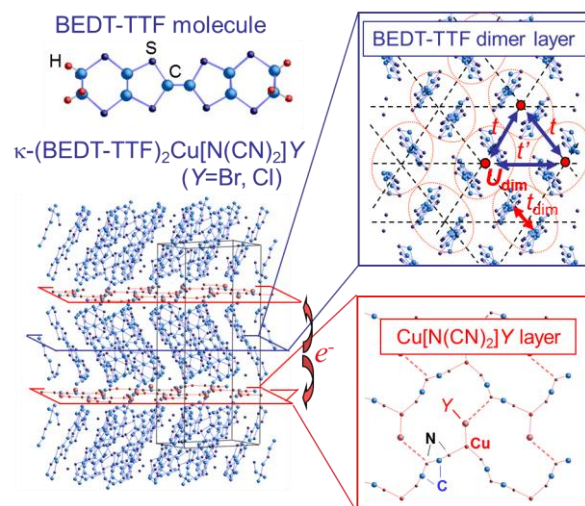
---

## 1. Introduction

Metal-insulator (MI) transition is an important research subject on electronic properties in solid state physics. Among the various types of MI transitions, the Mott transition due to electron-electron interactions is one of the most attractive phenomenon [1]. After discovery of the high- $T_c$  copper oxides, the Mott insulating state realized in non-doped parent compounds has become

one of the leading vehicles for the study of strongly correlated electron systems [2]. Another way of MI transition caused by electron localization originates from the interference of electron wave functions due to randomness. This is the Anderson localization insulator, derived by introducing disorder into the crystal [3,4]. For more than half a century, many active researches have been conducted theoretically and experimentally since P. W. Anderson propounded the concept in 1958 [3–5]. Since randomness in the correlated electron system is essentially important in real materials, systematic studies of disorder and randomness effects are desired in systems near to a Mott transition in order to understand their physical properties. In the course of investigation of high- $T_c$  copper oxides, the carrier doping to the parent Mott insulators brought to light the problems involved in randomness for the correlated electrons [2]. A similar situation may occur in the study of the Anderson localization in doped semiconductors. In this way of controlling the carrier number, randomness introduced by either partially substituting the atoms having different valence or introducing deficiency on the atom sites is unavoidable in the experimental investigation of real materials.

**Figure 1.** Crystal structure of  $\kappa$ -(BEDT-TTF) $_2$ Cu[N(CN) $_2$ ]Y (Y = Br or Cl). The two-dimensional conduction plane consists of bis(ethylenedithio)-tetrathiafulvalene (BEDT-TTF) molecule dimers, which form an anisotropic triangular lattice. The anisotropy is defined by the ratio of the interdimer transfer energies  $t$  and  $t'$ . The degree of electron correlations is determined by the ratio of on-site (dimer) Coulomb energy  $U_{\text{dim}}$  to the bandwidth  $W$  ( $\sim 4t$ ).



Organic charge-transfer salts based on a donor molecule bis(ethylenedithio)-tetrathiafulvalene (abbreviated as BEDT-TTF or ET) have been recognized as being one of the most highly correlated electron systems [6,7]. Among them,  $\kappa$ -(BEDT-TTF) $_2$ X, where X is an anion, has attracted considerable attention as a bandwidth-controlled Mott transition system [8,9]. Its remarkable feature is that the native quarter filled band is modified to an effective half filled band by the strong dimer structure consisting of two BEDT-TTF molecules [8,9]. Especially, series of the salts  $\kappa$ -(BEDT-TTF) $_2$ Cu[N(CN) $_2$ ]Y (Y = Br or Cl) are known to be border materials near the Mott transition as shown in Figure 4 [7–10]. The crystal structure is depicted in Figure 1. The two-dimensional conduction plane consists of BEDT-TTF molecule dimers, which form an anisotropic triangular lattice. The intradimer

transfer energy  $t_{\text{dim}}$  is larger than the interdimer transfer energies  $t$  and  $t'$ . The anisotropy of the triangular lattice changes with the ratio  $t'/t$ . The ratio  $t'/t$  ranges from 0.7 in  $\kappa$ -(BEDT-TTF)<sub>2</sub>Cu[N(CN)<sub>2</sub>]Br to 1.1 in  $\kappa$ -(BEDT-TTF)<sub>2</sub>Cu<sub>2</sub>(CN)<sub>3</sub> on the basis of extended Hückel calculations [11,12]. The ratio,  $t'/t$ , can be considered as the parameter for the frustration of the triangular lattice. The value  $t' \approx t$  in  $\kappa$ -(BEDT-TTF)<sub>2</sub>Cu<sub>2</sub>(CN)<sub>3</sub> indicates the importance of the frustrations in the isotropic triangular lattice. A spin liquid ground state was found in  $\kappa$ -(BEDT-TTF)<sub>2</sub>Cu<sub>2</sub>(CN)<sub>3</sub> [13] and the origin has been discussed extensively on the basis of the isotropic triangular frustrations. A recent review on the frustration is found in the cited article [14].

In this strongly correlated electronic system, several electronic and magnetic phases appear and the transitions between these phases are controlled by the applied pressure and the slight chemical substitution of donor and anion molecules, which change the conduction band width  $W \sim 4t$  with respect to the effective Coulomb repulsion  $U_{\text{dim}}$  of a dimer. The value of  $U_{\text{dim}}$  can be estimated approximately as  $U_{\text{dim}} \sim 2t_{\text{dim}}$ . From this relation, the value of  $U_{\text{dim}}$  is about 0.4 eV for  $t_{\text{dim}} \sim 0.2$  eV. This value of  $U_{\text{dim}}$  is comparable to the bandwidth  $W \sim 4t$  and suggests that electron correlation effects are important. One can control the strength of the electron correlations relative to the bandwidth by applying low pressure or substituting molecules partially, which leads to a Mott insulator ( $Y = \text{Cl}$ )–metal/superconductor ( $Y = \text{Br}$ ) transition. Therefore, molecular conductors with strongly correlated electrons can become potential candidates for studying the randomness effect by developing an experimental method for introducing disorder into crystals without modifying the electronic states, but in which only scattering rates are changed.

Recently two groups have reported the band structures of  $\kappa$ -(BEDT-TTF)<sub>2</sub>X based on DFT calculations [15,16]. The ratios  $t'/t$  in their calculations are significantly smaller than those obtained by Hückel calculations. For example,  $t'/t = 0.8$  in  $\kappa$ -(BEDT-TTF)<sub>2</sub>Cu<sub>2</sub>(CN)<sub>3</sub> on the basis of the DFT calculations [15,16] is far from the value ( $t'/t = 1.1$ ) obtained by the extended Hückel calculations [12]. In addition, there are large differences in the evaluation of  $U$  of  $\kappa$ -(BEDT-TTF)<sub>2</sub>X among the different calculations and experiments [15–17]. The current situation together with discussions on the parameters  $t$ ,  $U$ ,  $V$  and the correlated electronic states are found in a recent review article [14].

There have been several investigations on the disorder effect in molecular conductors [18–26]. The disorder was introduced in many cases by controlling the sample cooling speed for changing the level of the conformational disorder of the terminal ethylene groups of BEDT-TTF [24–26] and in some cases by partial molecular substitution [21–23]. In addition, it is known that X-ray irradiation to the organic materials can cause molecular defects and disorder [18–20,27]. Actually, the molecular disorder introduced by X-ray irradiation to the organic superconductor  $\kappa$ -(BEDT-TTF)<sub>2</sub>Cu(NCS)<sub>2</sub> increases the residual resistivity, and suppresses the superconductivity [18,27]. We investigated the X-ray irradiation effect widely in  $\kappa$ -(BEDT-TTF)<sub>2</sub>X showing superconductivity or Mott insulating state from the viewpoint of the relation between the correlated electronic states and randomness [20,27–34]. Recently, we found that the weak molecular disorder introduced by X-ray irradiation of the organic superconductor  $\kappa$ -(BEDT-TTF)<sub>2</sub>Cu[N(CN)<sub>2</sub>]Br induced the Anderson-type localization insulating state from the strongly correlated metallic/superconducting state [31].

In this paper, we present our recent studies on the randomness effect on the correlated electrons near the Mott transition in the dimer-Mott system  $\kappa$ -(BEDT-TTF)<sub>2</sub>X. Randomness is introduced by X-ray irradiation which does not modulate the electronic states but only the scattering. First, we show

how molecular defects and disorder are introduced by X-ray irradiation. Second, we mention the nature of the defects and disorder caused by the X-ray irradiation. Finally the randomness effect on the electronic properties near the Mott transition is discussed on the basis of the concept of the Mott-Anderson transition with the proposal of an electronic phase diagram including the parameter of randomness.

## 2. Results and Discussion

### 2.1. X-ray Irradiation to the Molecular Conductors: Molecular Defects

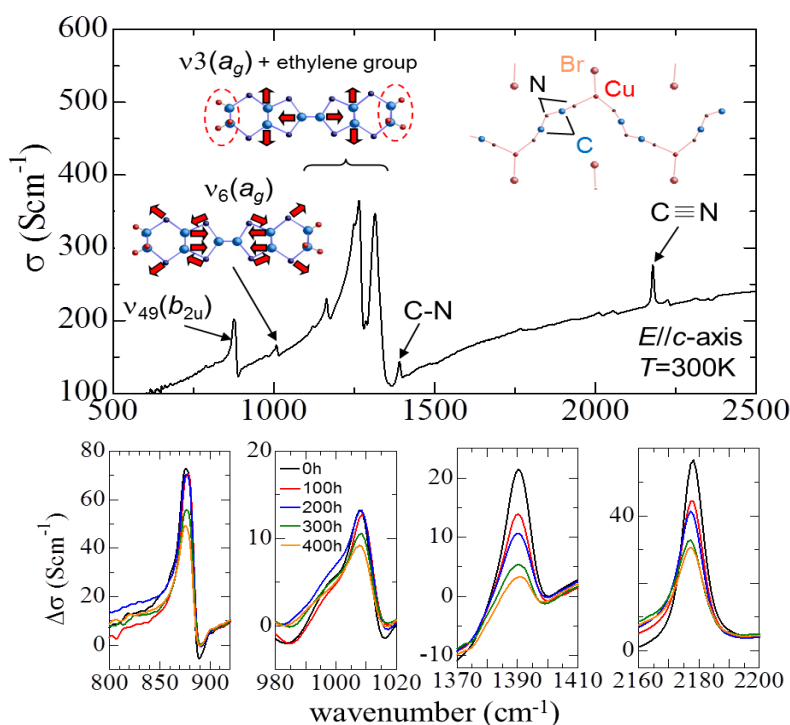
X-ray irradiation of the organic materials has been considered as introducing molecular defects which are radiolysed by ionizing radiation [35]. This kind of molecular defect remains in the crystal permanently, while the irradiation damage in inorganic materials, in general, is caused by atomic displacement from the regular sites, which can be restored by an appropriate heat treatment. The average volume of the molecular defect has been considered to be of the order of one molecular volume. Such molecular damage has been recognized empirically by observing a diffraction spot which becomes gradually unclear with exposure time in the X-ray crystal structure analysis experiments. Such molecular defects in the organic conductors act as a scattering center for the conduction electrons, resulting in the increase of the residual resistivity at low temperature [36]. In the case of low dimensional conductors such as one-dimensional charge transfer salts, for example,  $(\text{TMTSF})_2\text{X}$ , the defects divide the conducting chains into segments [35,37]. Then the density wave states are suppressed and destroyed by irradiation [35,38,39].

For X-ray irradiation of the charge transfer salts consisting of donor and anion molecules, it is not clear which parts of the molecules are damaged predominantly by the irradiation. In the early stage of our study, we expected that the molecular defects were formed at the BEDT-TTF donor molecule site because a large decrease of the resistivity was observed during the irradiation at room temperature [20]. The reduction of the resistivity might be caused by an effective carrier doping to a Mott insulating state due to a local imbalance of the charge transfer in the crystal. As mentioned later in this section, however, recent progress in our study on the molecular defect site and randomness effect on electronic states suggests that the defects are introduced mainly in the anion molecule layer [27,32,33] and the decrease of resistivity does not indicate change of the carrier number [27]. The behavior of the resistivity results from a transition from the gapped Mott insulator to the soft Coulomb (Hubbard) gapped localization insulator in which randomness introduces a finite density of states at the Fermi level into the strongly correlated electron system.

To determine the defect sites in the molecular crystal, the irradiation dose dependence of the molecular vibration modes was measured by means of infrared optical reflectance experiments at 300 K [32,33]. Most of the molecular vibration modes of both donor and anion molecules appear in the mid-infrared region. Thus the photon energy region is called a finger-print region because the rich information of the molecules and molecular crystals is contained in the molecular vibration modes of the spectra. Figure 2 shows the infrared optical conductivity ( $E//c$ -axis) at 300 K in the finger-print photon energy region of  $\kappa$ -(BEDT-TTF) $_2$ Cu[N(CN) $_2$ ]Br [33]. Peak structures at approximately 880 and 1010  $\text{cm}^{-1}$  are assigned to the  $\nu_{49}(b_{2u})$  and  $\nu_6(a_g)$  modes of the BEDT-TTF intramolecular vibrations, respectively. The amplitude of these vibration modes is relatively insensitive to the irradiation dose.

On the other hand, the peak signals at approximately 1390 and 2180  $\text{cm}^{-1}$ , which are assigned to the vibration modes related to the dicyanamide group of the anion molecule [40], are significantly suppressed by irradiation. Particularly, the mode at 1390  $\text{cm}^{-1}$ , which originates from the CN single bonding, shows marked reduction. We note that no alternate vibration mode between 500–3000  $\text{cm}^{-1}$  appears after irradiation. These changes in the molecular vibration modes by X-ray irradiation were observed similarly in the Mott insulator salt,  $\kappa$ -(BEDT-TTF)<sub>2</sub>Cu[N(CN)<sub>2</sub>]Cl [32]. The organic salts are composed of light-weight elements except for the copper atoms in the anion molecules. Larger X-ray absorption is expected at the copper site of the anion molecule than that at the other light-weight element sites. The dicyanoamide groups coordinated to the copper may be strongly influenced by X-ray irradiation. Therefore we expect that the major molecular defects are created in the anion molecule layers by X-ray irradiation, and the carriers in the BEDT-TTF layers are influenced by the random potential modulation from defects in the anion layer.

**Figure 2.** The infrared optical conductivity ( $E//c$ -axis) in the finger-print photon energy region of  $\kappa$ -(BEDT-TTF)<sub>2</sub>Cu[N(CN)<sub>2</sub>]Br at 300 K [33]. In the lower figures, changes of the molecular vibration modes with X-ray irradiation are shown after subtracting the smooth background of  $\sigma(\omega)$ .

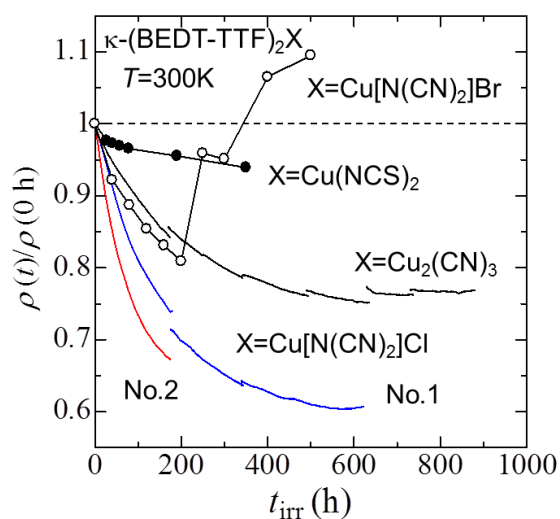


## 2.2. Resistance Change by X-ray Irradiation at Room Temperature

The resistivity of  $\kappa$ -(BEDT-TTF)<sub>2</sub>X samples during X-ray irradiation at room temperature changes with the irradiation time [20]. Figure 3 shows the irradiation time dependence of the resistivity of  $\kappa$ -(BEDT-TTF)<sub>2</sub>X at 300 K. All superconductors ( $X = \text{Cu}(\text{NCS})_2$  and  $\text{Cu}[\text{N}(\text{CN})_2]\text{Br}$ ), and insulators ( $X = \text{Cu}[\text{N}(\text{CN})_2]\text{Cl}$  and  $\text{Cu}_2(\text{CN})_3$ ) show a substantial reduction in resistivity. Among them, the Mott insulators with  $X = \text{Cu}[\text{N}(\text{CN})_2]\text{Cl}$  and  $\text{Cu}_2(\text{CN})_3$  show a more significant decrease in resistivity in comparison with that in the superconductor  $X = \text{Cu}(\text{NCS})_2$ . In both insulators, the resistivity decreases

rapidly with the initial irradiation, and then tends to become saturated. After several hundred hours irradiation, the resistivity reaches a minimum and then increases slightly. These features are qualitatively the same in both cases when using copper and tungsten targets although the former contains characteristic  $K_\alpha$  radiation and the latter does not. Unlike smooth changes in the Mott insulators, strange behavior of the resistivity is observed in the superconductor  $X = \text{Cu}[\text{N}(\text{CN})_2]\text{Br}$ . In the initial stage of the irradiation below 200 h, the rapid reduction in the resistivity is similar to that in  $X = \text{Cu}[\text{N}(\text{CN})_2]\text{Cl}$  and  $\text{Cu}_2(\text{CN})_3$ . However, further irradiation leads to increase in the resistivity above approximately 200 h irradiation. This anomalous resistivity behavior is closely related to the critical randomness of localizing insulating states discussed in the latter section [31].

**Figure 3.** X-ray irradiation time dependence of the in-plane resistivity of  $\kappa\text{-(BEDT-TTF)}_2X$  at 300 K [20]. Each resistivity curve is normalized by the value before the irradiation.

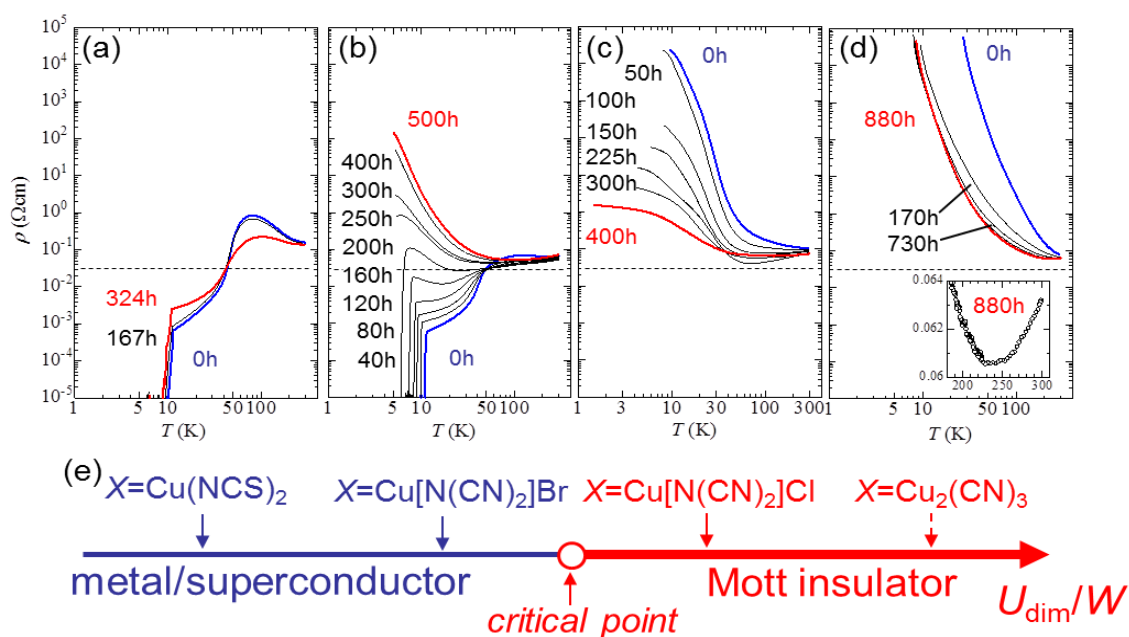


### 2.3. Temperature Dependence of the Resistivity of $\kappa\text{-(BEDT-TTF)}_2X$ Irradiated by X-ray

Figure 4 shows the temperature dependence of  $\kappa\text{-(BEDT-TTF)}_2X$  with  $X = \text{Cu}(\text{NCS})_2$ ,  $\text{Cu}[\text{N}(\text{CN})_2]\text{Br}$ ,  $\text{Cu}[\text{N}(\text{CN})_2]\text{Cl}$  and  $\text{Cu}_2(\text{CN})_3$  irradiated by X-ray. At the start with the superconductor  $X = \text{Cu}(\text{NCS})_2$  and  $\text{Cu}[\text{N}(\text{CN})_2]\text{Br}$  before irradiation, the resistivity shows the characteristic behavior reported previously [41]: a broad resistivity hump at 100 K, a crossover around  $T^*$  from a bad to good metallic state at low temperature where the resistivity follows  $\rho(T) = \rho_0 + AT^2$  and the superconducting transition at  $T_c \sim 10$  K ( $X = \text{Cu}(\text{NCS})_2$ ) and 11 K ( $X = \text{Cu}[\text{N}(\text{CN})_2]\text{Br}$ ). However, X-ray irradiation of the samples changes the behavior of the resistivity drastically. In the case of the  $X = \text{Cu}(\text{NCS})_2$  sample, the characteristic hump structure around 100 K is suppressed [18] and the  $\rho(T)$  curves intersect a single point at approximately  $T = 50$  K and  $\rho \sim 30$  mΩ cm. These changes are reproduced well in line with the previous report on the inter-plane resistivity measurements [18]. In contrast to the  $X = \text{Cu}(\text{NCS})_2$  sample, a rather low irradiation dose for the  $X = \text{Cu}[\text{N}(\text{CN})_2]\text{Br}$  sample induces a drastic change of the temperature dependence of the resistivity [31]. The resistivity hump at 100 K is completely suppressed and the residual resistivity  $\rho_0$  increases rapidly with the irradiation time. The intersection point at  $T = 50$  K and  $\rho \sim 30$  mΩ cm is the same as that in the irradiated  $X = \text{Cu}(\text{NCS})_2$  sample. At  $t_{\text{irr}} = 200$  h,  $\rho(T)$  shows an almost temperature independent behavior at the same resistivity range of the intersection

point. It is to be noted that such a critical irradiation time of 200 h is also seen in the anomalous change of  $\rho$  at room temperature as shown in Figure 3. At  $t_{\text{irr}} > 250$  h,  $\rho(T)$  curves show an insulating behavior at low temperature and the curves do not cross the intersection point. At  $t_{\text{irr}} = 500$  h at last, the resistivity at 4 K becomes more than five orders of magnitude larger than  $\rho_0$  before irradiation. The change of the resistivity clearly indicates that the observed MI transition is induced by disorder introduced by X-ray irradiation. In the later section, we will discuss the insulating localized electron states of an X-ray irradiated  $X = \text{Cu}[\text{N}(\text{CN})_2]\text{Br}$  sample.

**Figure 4.** Temperature dependence of the resistivity of  $\kappa\text{-(BEDT-TTF)}_2X$ , (a)  $X = \text{Cu}(\text{NCS})_2$ ; (b)  $\text{Cu}[\text{N}(\text{CN})_2]\text{Br}$ ; (c)  $\text{Cu}[\text{N}(\text{CN})_2]\text{Cl}$  and (d)  $\text{Cu}_2(\text{CN})_3$  irradiated by X-ray. The time indicated in each figure is the total X-ray exposure time at room temperature; (e) Schematic phase diagram in  $\kappa\text{-(BEDT-TTF)}_2X$  for  $U_{\text{dim}}/W$ .



Before irradiation both of the Mott insulators  $X\text{Cu}[\text{N}(\text{CN})_2]\text{Cl}$  and  $\text{Cu}_2(\text{CN})_3$  show an activation type behavior of the resistivity as has been reported previously [20]. With increasing the irradiation dose, the resistivity decreases in the whole temperature range. It is noted, moreover, that a metal-like temperature dependence appears in  $X = \text{Cu}[\text{N}(\text{CN})_2]\text{Cl}$  with a rather small irradiation dose. The resistivity decreases sublinearly with lowering temperature down to about 50 K, and then it changes and increases rapidly. The temperature of about 50 K corresponds also to the characteristic temperature in the non-irradiated sample at which the activation energy obtained from the Arrhenius plots of the resistivity changes and the charge gap found in the optical measurements starts to grow [42]. The temperature region where the metal-like behavior is observed, however, does not extend below 50 K on increasing the irradiation dose. Finally, the sample irradiated for 400 h changes to show an increase in resistivity at low temperatures and concurrently the metal-like behavior of the resistivity becomes weak. In  $X = \text{Cu}_2(\text{CN})_3$ , the resistivity also decreases with the irradiation time. However, it takes a large irradiation dose to observe the metal-like behavior of the resistivity which is only in a narrow temperature region above about 230 K as shown in the inset.

In this manner, randomness from the molecular defects introduced by X-ray irradiation strongly affects the electronic states of  $\kappa$ -(BEDT-TTF)<sub>2</sub>X. The effect becomes significant especially in  $\kappa$ -(BEDT-TTF)<sub>2</sub>Cu[N(CN)<sub>2</sub>]Y with (Y = Br and Cl) which is in the vicinity of the critical point for the Mott transition.

#### 2.4. Electron Localization by Randomness in $\kappa$ -(BEDT-TTF)<sub>2</sub>Cu[N(CN)<sub>2</sub>]Br

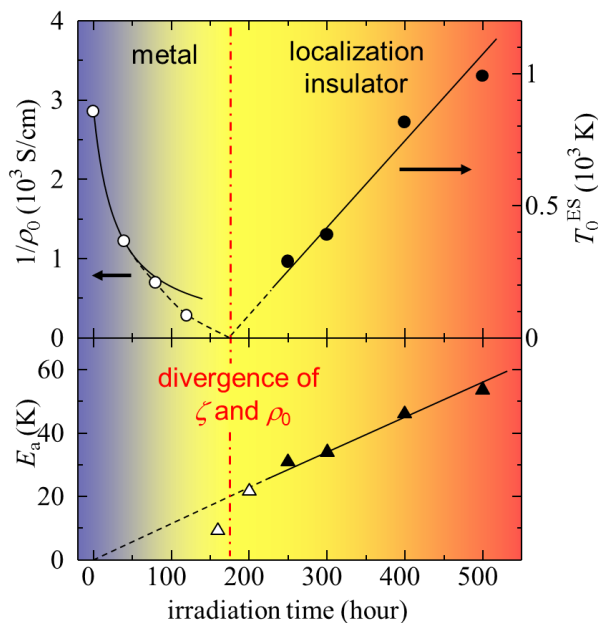
In this section, we focus on the randomness effect in the insulating state of the X-ray irradiated  $\kappa$ -(BEDT-TTF)<sub>2</sub>Cu[N(CN)<sub>2</sub>]Br, which shows a localization MI transition induced by disorder [31,33]. In the insulating temperature region (10 K < T < 40 K) with  $t_{\text{irr}} > 200$  h (Figure 4b), the resistivity follows accurately the Arrhenius law described as  $\rho(T) = \rho_a \exp(E_a/k_B T)$ , where  $\rho_a$  is the resistivity extrapolated to the high-temperature limit and  $E_a$  is the characteristic energy. The Arrhenius-type temperature dependence usually appears in band insulators (semiconductors) and  $E_a$  corresponds to the band gap energy. The present results, however, do not originate from a thermal activation across a band-gap, but from electron hopping between nearest-neighbor localized sites in the disordered system at high temperature [1]. This is demonstrated by the downward deviation of the resistivity from the Arrhenius law at lower temperature, which is not expected in a band-gap insulator. The energy  $E_a$  in the hopping conduction corresponds to the degree of randomness. As shown in the lower part of Figure 5,  $E_a$  at  $t_{\text{irr}} > 200$  h increases linearly with  $t_{\text{irr}}$  and the extrapolation to lower irradiation times suggests an intersect with the origin. At  $t_{\text{irr}} < 200$  h (open triangles), there are some deviations from the linear dependence. This may be due to the intermediate behavior between insulator and metal. Actually,  $\rho(T)$  shows the  $\log(T)$  dependence in the intermediate irradiation at  $t_{\text{irr}} = 160$ –200 h, which suggests weak localization behavior in the metallic side for the MI transition. The extrapolated value of  $\rho_a \sim 20$  mΩ cm in the high-temperature limit is reasonably close to the nearly temperature-independent resistivity at  $t_{\text{irr}} = 200$  h. Here, we estimate the corresponding sheet resistance of 130 kΩ from  $\rho_a$  assuming a layer distance of 1.5 nm. This value is comparable to the inverse of the minimum conductivity in two dimensions [43],  $\sigma_{\text{min}} \sim 0.1e^2/h \sim 2.4 \times 10^{-5}$  S, and then  $1/\sigma_{\text{min}} \sim 40$  kΩ. The fairly good correspondence even though a rough estimation could suggest that the observations of  $\rho_a$  and temperature independent resistivity show the features of critical resistivity for the MI transition induced by disorder. At the same time, the resistivity ( $\sim 30$  mΩ cm) at the intersection point of  $\rho(T)$  curves is also close to  $\rho_a$ .

The resistivity below about 10 K deviates from the Arrhenius law and can be fitted to the following function,  $\rho(T) = \rho_h \exp[(T_0/T)^n]$ , where  $n = 1/3$  is expected for variable range hopping (VRH) in two dimensions, and  $1/4$  in three dimensions [1]. The case where  $n = 1/2$  was known to appear in localized states in the presence of long-range Coulomb repulsive interactions, which was proposed by Efros and Shklovskii (ES) [44]. This being the case then it leads to the formation of a Coulomb gap. The results fit fairly well, all values of  $n = 1/2$ ,  $1/3$  and  $1/4$  are equally good. Considering the strong two-dimensionality and the strong electron correlation in this material, however, VRH in two dimensions (2D-VRH) or the ES model should be validated. We examined the insulating behavior in  $\rho(T)$  by considering weak localization including electron-electron interactions [45,46], in addition to a model including short-range Coulomb interactions with disorder by Shinaoka and Imada (SI) [47,48]. The former, however, does not fit to the observed exponential increase of  $\rho(T)$  since it modifies only

the prefactor of the  $\log(T)$  term in  $\rho(T)$ . At low temperature, all values of ES, 2D-VRH and SI coincide with each other. On the other hand, the Arrhenius law is applicable at high temperatures. In the intermediate region, SI may offer a better description than ES and 2D-VRH. The crossover from SI at higher temperatures to ES or 2D-VRH at lower temperatures is simply understood by changing the range of Coulomb interactions from short-range to long-range due to weak electron screening capability with decreasing temperature.

The critical property appears as a divergence of the localization length  $\xi$ . The temperature coefficient  $T_0$  is related to  $\xi$  as  $k_B T_0^{\text{ES}} \sim e^2/\kappa\xi$  in the case of ES [44], where  $\kappa$  is the dielectric constant. Figure 5 shows the critical behavior of  $\rho_0$  and  $\xi$  for the MI transition as a function of  $t_{\text{irr}}$ . In the insulator region,  $T_0^{\text{ES}}$  increases almost linearly with  $t_{\text{irr}}$ . One could obtain a critical irradiation time of 150–200 h from the extrapolation to  $T_0^{\text{ES}}(t_{\text{irr}}) = 0$  at which the localization length diverges. The value of  $\xi$  could be estimated to be in the range of 0.2–2 nm at  $t_{\text{irr}} = 500$  h if we assumed  $\kappa = 10$ –100 although the dielectric properties of the present irradiated sample have not been measured so far. The estimated value is reasonably consistent with the site hopping scenario of ES and VRH in comparison to the mean distance ( $\sim 0.3$  nm) of BEDT-TTF molecules. On the other hand, the inverse of  $\rho_0$  can be plotted in the metal region. The extrapolation of  $1/\rho_0$  goes to zero at  $t_{\text{irr}} \sim 150$ –200 h. The critical behavior for  $\xi$  and  $\rho_0$  with a convergence at a single  $t_{\text{irr}} = 150$ –200 h from both insulator and metal sides strongly supports that there is a critical disorder for the MI transition.

**Figure 5.** Irradiation time dependence of the residual resistivity  $\rho_0$  of  $\kappa$ -(BEDT-TTF)<sub>2</sub>Cu[N(CN)<sub>2</sub>]Br,  $T_0^{\text{ES}}$  in the ES model and  $E_a$  in the Arrhenius law. Solid curve for  $1/\rho_0$  represents the linear dependence of  $\rho_0(t_{\text{irr}})$ .

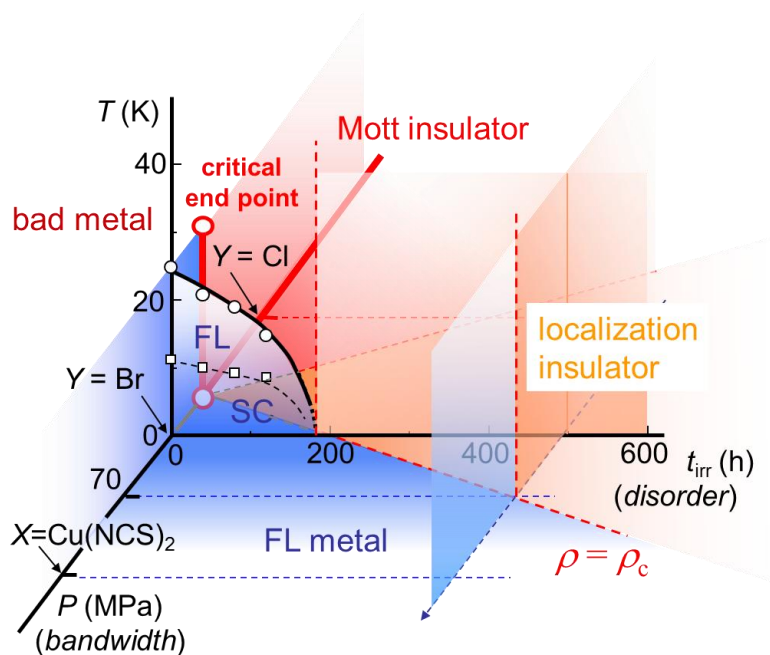


It is important to examine the pressure effect in order to consider the relation between electron correlations and disorder. With increasing pressure, the resistivity decreases and the insulating behavior become weaker [31]. After going through the resistivity level of the same order as the critical resistivity for the MI transition, weak localization behavior is found below approximately 10 K at 70–90 MPa and then metallic behavior is restored at 150–200 MPa. In this process, pressure broadens

the band width  $W$  in comparison to the on-site Coulomb energy  $U_{\text{dim}}$  resulting in weaker electron correlations. At the same time, the amount of disorder is not essentially influenced by pressure.

A schematic electronic phase diagram with the axes of temperature, band width and disorder is depicted in Figure 6 [31,33]. The present  $X = \text{Cu}[\text{N}(\text{CN})_2]Y$  ( $Y = \text{Br}$  and  $\text{Cl}$ ) samples are located near to the Mott transition on the metallic and Mott insulator sides, respectively. The introduction of disorder changes the metal to an Anderson-type localization insulator after crossing a critical disorder value characterized by the minimum conductivity. Then the broader  $W$  induced by pressure brings the insulator back to the metallic state at the same minimum conductivity. This schematic phase diagram for disorder accurately represents the experimental observation. In addition, the phase diagram may explain why the other organic superconductor  $X = \text{Cu}(\text{NCS})_2$  does not show an insulating behavior but only an increase in residual resistivity although almost the same level of disorder is introduced in the same way with X-ray irradiation. In this case, the electron correlation is not strong enough to cause localization of carriers with the same amount of disorder in comparison to  $X = \text{Cu}[\text{N}(\text{CN})_2]\text{Br}$ . In theory, several phase diagram calculations based on the disordered Hubbard model have been reported [47–53]. Further considerations of the phase diagram are necessary to enable theoretical understanding in the future.

**Figure 6.** Schematic electronic phase diagram of  $\kappa\text{-(BEDT-TTF)}_2X$  for temperature  $T$ , irradiation time  $t_{\text{irr}}$  and pressure  $P$ . The thick dashed red lines indicate the critical resistivity  $\rho_c$  between the metal (FL) and the localization insulator. The temperature dependence of the resistivity shows a  $T^2$  dependence in the FL metal [33].



### 2.5. Infrared Spectroscopy of the Localization Insulating State

In principle, a localization insulator has a finite value for the density of states at the Fermi level and the electrons near the Fermi level are localized, while the Mott insulator has no density of states at the Fermi level due to opening of the Mott gap by electron correlation. Near the critical point of the Mott

transition tuned by the bandwidth, the randomness on the Mott insulating side may cause the Coulomb soft gap state [44,47,48]. On the other hand, as shown in Figure 7 schematically, randomness on the metal side induces an Anderson localization insulator as has been found in  $\kappa$ -(BEDT-TTF)<sub>2</sub>Cu[N(CN)<sub>2</sub>]Br irradiated by X-rays. In order to obtain detailed information on the electronic states of the Mott-Anderson transition, a spectroscopic study near the Fermi level is important.

**Figure 7.** Schematic figure of the density of states at the Fermi level of  $\kappa$ -(BEDT-TTF)<sub>2</sub>Cu[N(CN)<sub>2</sub>]Y. The electronic state very near the Mott transition with randomness is not so clear. A gapless localization state, *i.e.*, soft Coulomb gapped state, is expected.

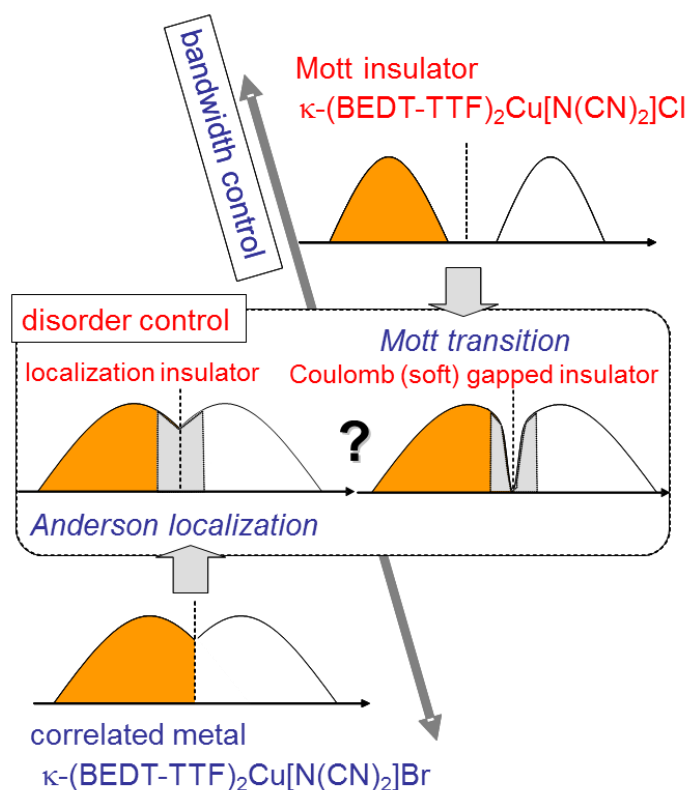
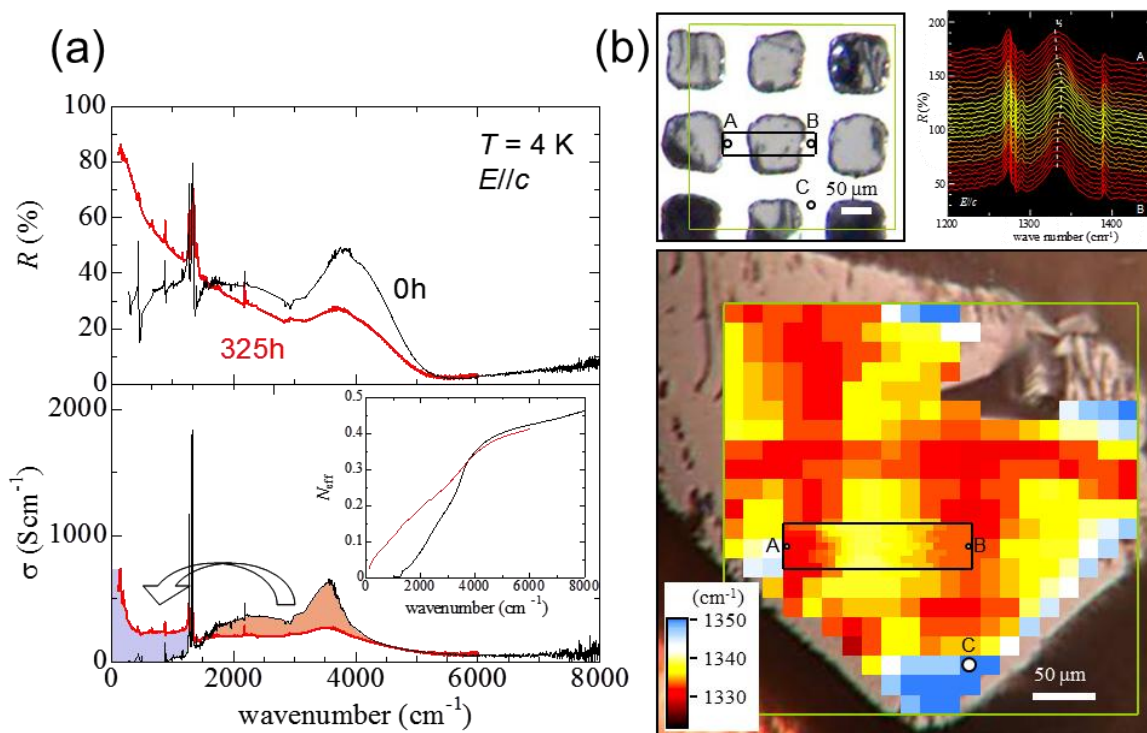


Figure 8a shows the optical reflectivity and conductivity spectra at 4 K in  $E//c$ -axis of  $X = \text{Cu}[\text{N}(\text{CN})_2]\text{Cl}$  before and after 325 h X-ray irradiation [30]. The spectra of non-irradiated  $X = \text{Cu}[\text{N}(\text{CN})_2]\text{Cl}$  was qualitatively in good agreement with results of previous reports [42,54–56]. Broad absorption peaks at  $2250 \text{ cm}^{-1}$  and  $3350 \text{ cm}^{-1}$  were attributed to interband transitions in the Mott-Hubbard bands and dimer bands, respectively [56]. In addition, an optical gap corresponding to a Hubbard gap appeared, approximately below  $1000 \text{ cm}^{-1}$  [42]. The magnitude of the interband transitions is reduced by X-ray irradiation. The conductivity of the broad absorption peaks decreases with increasing irradiation time (the spectra at the other irradiation times are not shown here). It should be noted that the irradiation did not induce the change of the absorption peak wavenumbers which correspond to the interband transition energies. This means that the fundamental electronic parameters, *i.e.*, the intra-dimer transfer energy and the effective Coulomb energy of the dimer site are not affected by X-ray irradiation. The reduction in the spectral weight (SW) in the mid-IR region due to irradiation was compensated by the shift of the SW to the far-IR region. Thus, the SW in the Mott-Hubbard gap increased with the irradiation time. We considered the randomness effect for the SW transfer from the

interband transitions to the low energy region. Inhomogeneity often leads to electron localization. Electron localizations in metals may shift the SW of the Drude peak to regions with high energy [57]. The behavior of the far-IR conductivity suggests that the weakly disordered metal state with a Coulomb gap, in which electron-electron interactions occur, is induced from the Mott insulating state by X-ray irradiation. We see an isosbestic point of the SW transfer at  $\sim 1700\text{ cm}^{-1}$ . In order to quantitatively evaluate the SW transfer by X-ray irradiation, we define the effective number of carriers as  $N_{\text{eff}}(\omega) = (2m_0)/(e^2N)\int\sigma(\omega')d\omega'$ , where  $m_0$  is the free electron mass and  $N$  is the number of BEDT-TTF dimers per unit volume. The inset of the lower panel in Figure 8 shows the effective carrier number  $N_{\text{eff}}(\omega)$  of X-ray irradiated  $X = \text{Cu}[\text{N}(\text{CN})_2]\text{Cl}$  at 4 K. The  $\omega$  dependence of  $N_{\text{eff}}$  shows how the SW is redistributed on increasing irradiation time. In the high energy region,  $N_{\text{eff}}$  tends to saturation so as to approach the value of 0.45–0.5. The saturation value is nearly independent of the irradiation time, which means the sum of the SWs is nearly conserved even with changing the IR spectra by X-ray irradiation. These features suggest that randomness by X-ray irradiation fills the Mott gap by the SW transfer from the interband transition. But no-Drude response and high dc resistivity indicate that the system is still in the insulating state. We may conclude that a Coulomb soft gapped insulating state as shown in Figure 7 is realized from the Mott insulator.

**Figure 8.** (a) Infrared optical reflectivity and conductivity of  $\kappa$ -(BEDT-TTF) $_2$ Cu[N(CN) $_2$ ]Cl before and after X-ray irradiation. The inset of the lower panel indicates the effective number of carriers  $N_{\text{eff}}$ ; (b) Scanning micro-region infrared reflectance spectroscopy (SMIS) scanning map of the partly X-ray irradiated  $X = \text{Cu}[\text{N}(\text{CN})_2]\text{Cl}$ . X-ray is irradiated to the sample through the molybdenum mesh mask.



We note finally in this section the possible applications of X-ray irradiation. By using an X-ray microbeam, we can fabricate low resistance circuits and dots in organic insulators. Actually

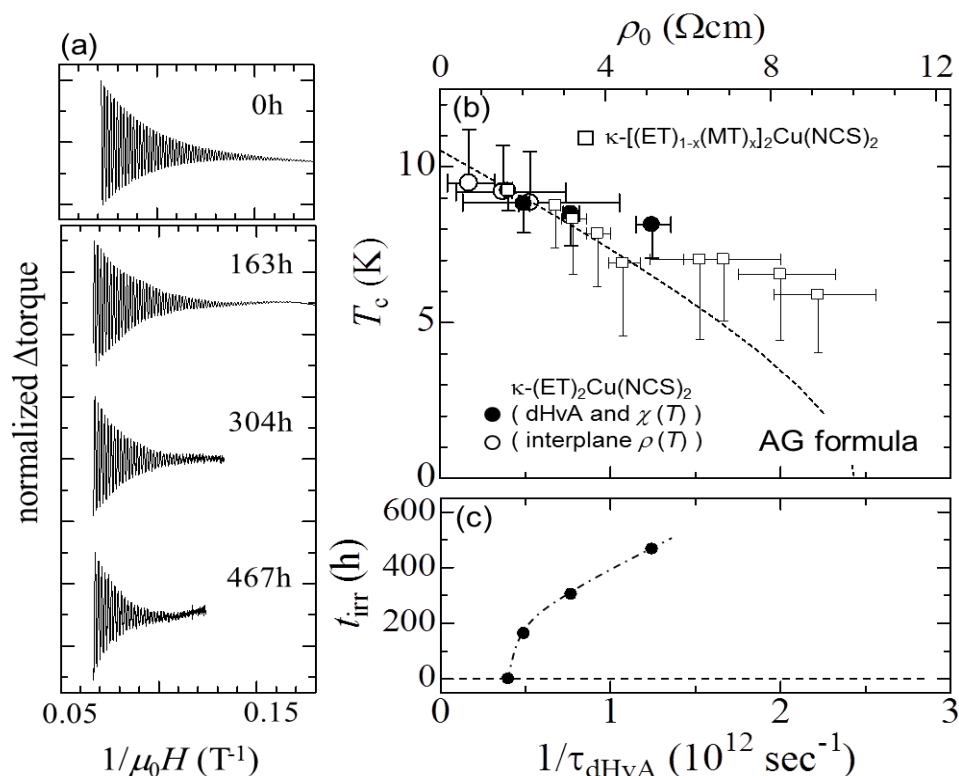
a low resistance pattern fabrication has been demonstrated as shown in Figure 8b [28]. The X-ray is irradiated through a mask of molybdenum mesh sheet (mesh size:  $90 \times 90 \mu\text{m}^2$ ) to  $\kappa\text{-(BEDT-TTF)}_2\text{Cu[N(CN)}_2\text{]Cl}$ . Scanning micro-region infrared reflectance spectroscopy (SMIS) [58,59] is performed to map space variation of the electronic states with a spatial interval of 15 or 5  $\mu\text{m}$ . The change of molecular vibration mode  $\nu_3$  of BEDT-TTF can indicate variation of the electronic states locally because the  $\nu_3$  mode markedly reflects the electronic state via electron molecular vibration coupling [55]. The main panel in Figure 8b shows the two-dimensional map of the frequency of the  $\nu_3$  mode. The brighter color indicates the low resistance (localized insulating state) where the X-ray is irradiated through the window of the mesh mask.

### 2.6. Scatterings by Randomness for Electrons in Metals and Superconductors

In order to evaluate quantitatively the randomness introduced by X-ray irradiation, the scattering time of the conduction electrons in the metallic state and the suppression of the superconductivity have been investigated [27]. The de Haas–van Alphen (dHvA) effect can evaluate microscopically the electronic states at the Fermi level [60]. The magnetic quantum oscillations at low temperature and high magnetic fields represent valuable information about the Fermi surface, the effective mass and the scattering time. For the organic metal/superconductor  $\kappa\text{-(BEDT-TTF)}_2\text{Cu(NCS)}_2$ , the size of the Fermi surface and the effective mass do not change much with X-ray irradiation. However, the scattering time which appears in the magnetic field dependence of the dHvA oscillation amplitude (Figure 9a) is strongly reduced by the X-ray irradiation as shown in Figure 9c. The potential modulation of the molecular defects in the anion layer, introduced by X-ray irradiation, may be the scattering center for conduction electrons in the BEDT-TTF layer. In addition, there was no indication of any magnetic impurity effect by the X-ray irradiation [27].

The suppression of the superconductivity by disorder is important in investigating superconductivity because it can give information on the pairing symmetry [61–64]. There have been several attempts to introduce disorder into organic superconductors, by creating molecular defects and impurities using electron, proton, and X-ray irradiation and anion or donor molecule substitution. By using the quantitatively evaluated scattering time from the dHvA study on the X-ray irradiated  $\kappa\text{-(BEDT-TTF)}_2\text{Cu(NCS)}_2$ , we discussed the suppression of superconductivity by introducing nonmagnetic disorder. As shown in Figure 9b, a large reduction in  $T_c$  with a linear dependence on  $1/\tau_{\text{dHvA}}$  is found in the small-disorder region below  $1/\tau_{\text{dHvA}} \sim 1 \times 10^{12} \text{ s}^{-1}$  in an X-ray-irradiated sample. The observed linear relation between  $T_c$  and  $1/\tau_{\text{dHvA}}$  is in agreement with the Abrikosov-Gor'kov (AG) formula [65], at least in the small-disorder region. This observation is reasonably consistent with the unconventional superconductivity proposed previously for the present organic superconductor [7,66,67].

**Figure 9.** (a) de Haas–van Alphen oscillations of  $\kappa$ -(BEDT-TTF)<sub>2</sub>Cu(NCS)<sub>2</sub> at 0.44 K before and after X-ray irradiation. The magnetic fields are applied perpendicularly to the conductive two-dimensional plane. The amplitude of the oscillations is normalized by the value of each oscillation at 14 T; (b) Relation between  $T_c$  and the inverse of the scattering time  $1/\tau_{\text{dHvA}}$ . In addition to the X-ray irradiated sample, the data of the partially BMDT-TTF (MT) molecule substituted sample is included for comparison. The dashed curve represents the Abrikosov-Gor’kov formula; and (c) The irradiation time dependence of the inverse of the scattering time  $1/\tau_{\text{dHvA}}$ .



### 3. Experimental Section

Single crystals of  $\kappa$ -(BEDT-TTF)<sub>2</sub>X with  $X = \text{Cu}(\text{NCS})_2$ ,  $\text{Cu}[\text{N}(\text{CN})_2]Y$  ( $Y = \text{Cl}$  and  $\text{Br}$ ) and  $\text{Cu}_2(\text{CN})_3$  were grown by the standard electrochemical oxidation method. The in-plane resistivity was measured by a conventional dc four-terminal method. The temperature dependence of the resistivity was measured at the same cooling rate of  $-0.4 \text{ K/min}$  in order to avoid a structural disorder effect due to fast cooling. The measurements under pressure were performed by using a standard piston cylinder-type clamp cell.

Samples were X-ray irradiated at 300 K by using a non-filtered tungsten tube with 40 kV and 20 mA. The corresponding dose rate was expected to be about 0.5 MGy/h following comparison with previous reports. During the irradiation, the resistivity was monitored as the irradiation time dependence. The irradiation time  $t_{\text{irr}}$  was the sum of multiple exposures at 300 K.

The polarized reflectance spectra in the mid-infrared region ( $600\text{--}8000 \text{ cm}^{-1}$ ) were measured along the electric field direction  $E$  parallel to the  $a$ -axis ( $E//a$ -axis) and the  $c$ -axis ( $E//c$ -axis) with a Fourier transform microscope-spectrometer. Synchrotron radiation light at BL43IR in SPring-8, Japan

Synchrotron Radiation Research Institute, was used for measurements in the far-IR region (100–600 cm<sup>-1</sup>). The reflectivity was determined by comparison with a thin gold film evaporated partly on the crystal surface. The optical conductivity was calculated by a Kramers-Kronig analysis of the reflectivity.

#### 4. Conclusions

We have presented the X-ray irradiation effect on the transport, optical and superconducting properties of the molecular conductors  $\kappa$ -(BEDT-TTF)<sub>2</sub>X, which is located near the Mott transition. Disorder introduced by X-ray irradiation changes the Fermi-liquid metal state of X = Cu[N(CN)<sub>2</sub>]Br to an Anderson-type localization insulating state and the Mott insulating state of X = Cu[N(CN)<sub>2</sub>]Cl to a Coulomb soft gapped insulating state. For improved understanding of the correlated electronic states with randomness approaching the Mott critical point, theoretical suggestions, for example in reference [68], in addition to experimental investigation are urgently needed in order to obtain a proper physical picture for the future. On the experimental side, spectroscopic investigations of more direct observations of the Coulomb gap state [69] will be the next challenge in the present molecular system.

#### Acknowledgments

This work has been carried out by collaboration with N. Yoneyama, N. Kobayashi, Y. Ikemoto, T. Moriwaki, H. Kimura, N. Toyota, K. Sano, H. Oizumi, Y. Nakamura, H. Sugawara, T. Nakamura and K. Furukawa. The author also thanks M. Lang, J. Müller, T. Nakamura, K. Miyagawa, K. Kanoda, H. Shinaoka, M. Imada, Y. Nishio, K. Yakushi, S. Iwai and S. Ishihara for valuable discussions.

A part of this work was performed at the High Field Laboratory for Superconducting Materials, IMR, Tohoku University. The SR experiments were performed at SPring-8 with the approval of JASRI. This work was partly supported by a Grant-in-Aid for Scientific Research (Nos. 20340085, 21110504, 23110702) from JSPS and MEXT, Japan.

#### References

1. Mott, N.F. *Metal–Insulator Transitions*; Taylor and Francis: London, UK, 1990.
2. Imada, M.; Fujimori, A.; Tokura, Y. Metal-insulator transitions. *Rev. Mod. Phys.* **1998**, *70*, 1039–1263.
3. Anderson, P.W. Absence of diffusion in certain random lattices. *Phys. Rev.* **1958**, *109*, 1492–1505.
4. Kramer, B.; MacKinnon, A. Localization: Theory and experiments. *Rep. Prog. Phys.* **1993**, *56*, doi:10.1088/0034-4885/56/12/001.
5. *50 Years of Anderson Localization*; Abrahams, E., Ed.; World Scientific Publishing Co. Pte. Ltd.: Singapore, 2010.
6. Ishiguro, T.; Yamaji, K.; Saito, G. *Organic Superconductors*, 2nd ed.; Springer-Verlag: Berlin, Germany, 1998.
7. Toyota, N.; Lang, M.; Müller, J. *Low-Dimensional Molecular Metals, Springer Series in Solid-State Sciences*; Springer-Verlag: Berlin, Germany, 2007; Volume 154.

8. Miyagawa, K.; Kanoda, K.; Kawamoto, A. NMR studies on two-dimensional molecular conductors: Mott transition in  $\kappa$ -(BEDT-TTF)<sub>2</sub>X. *Chem. Rev.* **2004**, *104*, 5635–5653.
9. Kanoda, K. Metal-insulator transition in  $\kappa$ -(ET)<sub>2</sub>X and (DCNQI)<sub>2</sub>M: Two contrasting manifestation of electron correlation. *J. Phys. Soc. Jpn.* **2006**, *75*, doi:10.1143/JPSJ.75.051007.
10. Sasaki, T.; Yoneyama, N.; Kobayashi, N. Mott transition and superconductivity in the strongly correlated organic superconductor  $\kappa$ -(BEDT-TTF)<sub>2</sub>Cu[N(CN)<sub>2</sub>]Br. *Phys. Rev. B* **2008**, *77*, 054505:1–054505:5.
11. McKenzie, R.H. A strongly correlated electron model for the layered organic superconductors  $\kappa$ -(BEDT-TTF)<sub>2</sub>X. *Comments Condens. Matter Phys.* **1998**, *18*, 309–337.
12. Komatsu, T.; Matsukawa, N.; Inoue, T.; Saito, G. Realization of superconductivity at ambient pressure by band-filling control in  $\kappa$ -(BEDT-TTF)<sub>2</sub>Cu<sub>2</sub>(CN)<sub>3</sub>. *J. Phys. Soc. Jpn.* **1996**, *65*, 1340–1354.
13. Shimizu, Y.; Miyagawa, K.; Kanoda, K.; Maesato, M.; Saito, G. Spin liquid state in an organic mott insulator with a triangular lattice. *Phys. Rev. Lett.* **2003**, *91*, 107001:1–107001:4.
14. Powell, B.J.; McKenzie, R.H. Quantum frustration in organic Mott insulators: From spin liquids to unconventional superconductors. *J. Phys. Cond. Matter* **2011**, *23*, doi:10.1088/0034-4885/23/5/056501.
15. Nakamura, K.; Yoshimoto, Y.; Kosugi, T.; Arita, R.; Imada, M. Ab initio derivation of low-energy model for  $\kappa$ -ET type organic conductors. *J. Phys. Soc. Jpn.* **2009**, *78*, doi:10.1143/JPSJ.78.083710.
16. Kandpal, H.C.; Opahle, I.; Zhang, Y.-Z.; Jeschke, H.O.; Valenti, R. Revision of model parameters for  $\kappa$ -type charge transfer salts: An Ab initio study. *Phys. Rev. Lett.* **2009**, *103*, 067004:1–067004:4.
17. Merino, J.; Dumm, M.; Drichko, N.; Dressel, M.; McKenzie, R.H. Quasiparticles at the verge of localization near the mott metal-insulator transition in a two-dimensional material. *Phys. Rev. Lett.* **2008**, *100*, doi:10.1103/PhysRevLett.100.086404.
18. Analytis, J.G.; Ardavan, A.; Blundell, S.J.; Owen, R.L.; Garman, E.F.; Jeynes, C.; Powell, B.J. Effect of irradiation-induced disorder on the conductivity and critical temperature of the organic superconductor  $\kappa$ -(BEDT-TTF)<sub>2</sub>Cu(SCN)<sub>2</sub>. *Phys. Rev. Lett.* **2006**, *96*, doi:10.1103/PhysRevLett.96.177002.
19. Babić, S.D.; Biškup, N.; Tomić, S.; Schweitzer, D. Electrical transport in the organic superconductor  $\beta$ -(BEDT-TTF)<sub>2</sub>AuI<sub>2</sub> [with BEDT-TTF = bis(ethylenedithio)tetrathiafulvalene]: Influence of x-ray-induced defects on the normal phase and superconducting ground state. *Phys. Rev. B* **1992**, *46*, 11765–11771.
20. Sasaki, T.; Oizumi, H.; Yoneyama, N.; Kobayashi, N. X-ray irradiation-induced carrier doping effects in organic Dimer–Mott insulators. *J. Phys. Soc. Jpn.* **2007**, *76*, doi:10.1143/JPSJ.76.123701.
21. Naito, T.; Bun, K.; Miyamoto, A.; Kobayashi, H.; Sawa, H.; Kato, R.; Kobayashi, A. Electrical and structural properties of  $\kappa$ -type organic conductor. *Synth. Met.* **1993**, *56*, 2234–2240.
22. Yoneyama, N.; Sasaki, T.; Kobayashi, N. Substitution effect by deuterated donors on superconductivity in  $\kappa$ -(BEDT-TTF)<sub>2</sub>Cu[N(CN)<sub>2</sub>]Br. *J. Phys. Soc. Jpn.* **2004**, *73*, 1434–1437.
23. Yoneyama, N.; Sasaki, T.; Oizumi, H.; Kobayashi, N. Impurity effect on superconducting properties in molecular substituted organic superconductor  $\kappa$ -(ET)<sub>2</sub>Cu(NCS)<sub>2</sub>. *J. Phys. Soc. Jpn.* **2007**, *76*, doi:10.1143/JPSJ.76.123705.

24. Stalcup, T.F.; Brooks, J.S.; Haddon, R.C. Temporal processes in a polymeric anion-based organic superconductor. *Phys. Rev. B* **1999**, *60*, 9309–9312.
25. Su, X.; Zuo, F.; Schlueter, J.A.; Kini, A.M.; Williams, J.M. 80 K anomaly and its effect on the superconducting and magnetic transition in deuterated  $\kappa$ -(BEDT-TTF)<sub>2</sub>Cu[N(CN)<sub>2</sub>]Br. *Phys. Rev. B* **1998**, *58*, 2944–2947.
26. Yoneyama, N.; Higashihara, A.; Sasaki, T.; Nojima, T.; Kobayashi, N. Impurity effect on the in-plane penetration depth of the organic superconductors  $\kappa$ -(BEDT-TTF)<sub>2</sub>X (X = Cu(NCS)<sub>2</sub> and Cu[N(CN)<sub>2</sub>]Br). *J. Phys. Soc. Jpn.* **2004**, *73*, 1290–1296.
27. Sasaki, T.; Oizumi, H.; Honda, Y.; Yoneyama, N.; Kobayashi, N. Suppression of superconductivity by nonmagnetic disorder in organic superconductor  $\kappa$ -(BEDT-TTF)<sub>2</sub>Cu(NCS)<sub>2</sub>. *J. Phys. Soc. Jpn.* **2011**, *80*, doi:10.1143/JPSJ.80.104703.
28. Yoneyama, N.; Sasaki, T.; Kobayashi, N.; Ikemoto, Y.; Moriwaki, T.; Kimura, H. Metallic pattern fabrication in organic Mott insulating crystal by local X-ray irradiation. *Solid State Commun.* **2009**, *149*, 775–777.
29. Yoneyama, N.; Furukawa, K.; Nakamura, T.; Sasaki, T.; Kobayashi, N. Magnetic properties of x-ray irradiated organic mott insulator  $\kappa$ -(BEDT-TTF)<sub>2</sub>Cu[N(CN)<sub>2</sub>]Cl. *J. Phys. Soc. Jpn.* **2010**, *79*, doi:10.1143/JPSJ.79.063706.
30. Sasaki, T.; Yoneyama, N.; Nakamura, Y.; Kobayashi, N.; Ikemoto, Y.; Moriwaki, T.; Kimura, H. Optical probe of carrier doping by x-ray irradiation in the organic dimer mott insulator  $\kappa$ -(BEDT-TTF)<sub>2</sub>Cu[N(CN)<sub>2</sub>]Cl. *Phys. Rev. Lett.* **2008**, *101*, doi:10.1103/PhysRevLett.101.206403.
31. Sano, K.; Sasaki, T.; Yoneyama, N.; Kobayashi, N. Electron localization near the Mott transition in the organic superconductor  $\kappa$ -(BEDT-TTF)<sub>2</sub>Cu[N(CN)<sub>2</sub>]Br. *Phys. Rev. Lett.* **2010**, *104*, 217003:1–217003:4.
32. Yoneyama, N.; Sasaki, T.; Kobayashi, N.; Furukawa, K.; Nakamura, T. X-ray irradiation effect on magnetic properties of Dimer–Mott insulators:  $\kappa$ -(BEDT-TTF)<sub>2</sub>Cu[N(CN)<sub>2</sub>]Cl and  $\beta'$ -(BEDT-TTF)<sub>2</sub>ICl<sub>2</sub>. *Phys. B* **2010**, *405*, S244–S246.
33. Sasaki, T.; Sano, K.; Sugawara, H.; Yoneyama, N.; Kobayashi, N. Influence of randomness on the Mott transition in  $\kappa$ -(BEDT-TTF)<sub>2</sub>X. *Phys. Status Solidi B* **2012**, doi:10.1002/pssb.201100614, in press.
34. Antal, Á.; Fehér, T.; Yoneyama, N.; Forró, L.; Sasaki, T.; Jánosy, A. Spin and charge transport in the X-ray irradiated quasi-2D layered compound  $\kappa$ -(BEDT-TTF)<sub>2</sub>Cu[N(CN)<sub>2</sub>]Cl. *Crystals* **2012**, in press.
35. Zuppiroli, L. Radiation damage in low dimensional conductors. *Radiat. Eff.* **1982**, *62*, 53–68.
36. Korin-Hamzić, B.; Forró, L.; Cooper, J.R.; Bechgaard, K. Magnetoresistance study of the effect of disorder on the organic superconductor bis-tetramethyltetraselenafulvalenium perchlorate. *Phys. Rev. B* **1988**, *38*, 11177–11183.
37. Zuppiroli, L.; Bouffard, S.; Bechgaard, K.; Hilti, B.; Mayer, C.W. Irradiation effects in quasi-one-dimensional organic conductors: The evidence of a transverse fixed-range phonon-assisted hopping. *Phys. Rev. B* **1980**, *22*, 6035–6043.
38. Choi, M.-Y.; Chaikin, P.M.; Huang, S.Z.; Haen, P.; Engler, E.M.; Greene, R.L. Effect of radiation damage on the metal-insulator transition and low-temperature transport in the tetramethyltetraselenofulvalinium PF<sub>6</sub> salt [(TMTSF)<sub>2</sub>PF<sub>6</sub>]. *Phys. Rev. B* **1982**, *25*, 6208–6217.

39. Forro, L.; Zuppiroli, L.; Pouget, J.P.; Bechgaard, K. X-ray diffuse-scattering study of the pinned charge-density waves in tetramethyltetraselenafulvalene dimethyltetracyanoquinodimethane (TMTSF-DMTCNQ) disordered by irradiation. *Phys. Rev. B* **1983**, *27*, 7600–7610.
40. Jürgens, B.; Höpfe, H.A.; Schnick, W. Synthesis, crystal structure, vibrational spectroscopy, and thermal behavior of lead dicyanamide  $\text{Pb}[\text{N}(\text{CN})_2]_2$ . *Solid State Sci.* **2002**, *4*, 821–825.
41. Strack, Ch.; Akinci, C.; Paschenko, V.; Wolf, B.; Uhrig, E.; Assmus, W.; Lang, M.; Schreuer, J.; Wiehl, L.; Schlueter, J.A.; *et al.* Resistivity studies under hydrostatic pressure on a low-resistance variant of the quasi-two-dimensional organic superconductor  $\kappa$ -(BEDT-TTF) $_2$ Cu[N(CN) $_2$ ]Br: Search for intrinsic scattering contributions. *Phys. Rev. B* **2005**, *72*, 054511:1–054511:10.
42. Kornelson, K.; Eldridge, J.E.; Wang, H.H.; Charlier, H.A.; Williams, J.M. Infrared study of the metal-insulator transition in the organic conductor  $\kappa$ -(BEDT-TTF) $_2$ Cu[N(CN) $_2$ ]Cl. *Solid State Commun.* **1992**, *81*, 343–349.
43. Ando, T.; Fowler, A.B.; Stern, F. Electronic properties of two-dimensional systems. *Rev. Mod. Phys.* **1982**, *54*, 437–672.
44. Efros, A.L.; Shklovskii, B.I. Coulomb gap and low temperature conductivity of disordered systems. *J. Phys. C* **1975**, *8*, L49–L51.
45. Altshuler, B.L.; Aronov, A.G.; Lee, P.A. Interaction effects in disordered fermi systems in two dimensions. *Phys. Rev. Lett.* **1980**, *44*, 1288–1291.
46. Fukuyama, H. Effects of interactions on non-metallic behaviors in two-dimensional disordered systems. *J. Phys. Soc. Jpn.* **1980**, *48*, 2169–2170.
47. Shinaoka, H.; Imada, M. Soft hubbard gaps in disordered itinerant models with short-range interaction. *Phys. Rev. Lett.* **2009**, *102*, doi:10.1103/PhysRevLett.102.016404.
48. Shinaoka, H.; Imada, M. Single-particle excitations under coexisting electron correlation and disorder: A numerical study of the Anderson–Hubbard model. *J. Phys. Soc. Jpn.* **2009**, *78*, doi:10.1143/JPSJ.78.094708.
49. Tanasković, D.; Dobrosavljević, V.; Abrahams, E.; Kotliar, G. Disorder screening in strongly correlated systems. *Phys. Rev. Lett.* **2003**, *91*, doi:10.1103/PhysRevLett.91.066603.
50. Byczuk, K.; Hofstetter, W.; Vollhardt, D. Mott–Hubbard transition versus Anderson localization in correlated electron systems with disorder. *Phys. Rev. Lett.* **2005**, *94*, doi:10.1103/PhysRevLett.94.056404.
51. Byczuk, K.; Hofstetter, W.; Vollhardt, D. Competition between Anderson localization and antiferromagnetism in correlated lattice fermion systems with disorder. *Phys. Rev. Lett.* **2009**, *102*, doi:10.1103/PhysRevLett.102.146403.
52. Aguiar, M.C.O.; Dobrosavljević, V.; Abrahams, E.; Kotliar, G. Critical behavior at the Mott–Anderson transition: A typical-medium theory perspective. *Phys. Rev. Lett.* **2009**, *102*, doi:10.1103/PhysRevLett.102.156402.
53. Farhoodfar, A.; Gooding, R.J.; Atkinson, W.A. Variational Monte Carlo study of Anderson localization in the Hubbard model. *Phys. Rev. B* **2011**, *84*, 205125:1–205125:7.
54. Eldridge, J.E.; Kornelsen, K.; Wang, H.H.; Williams, J.M.; Crouch, A.V.S.; Watkins, D.M. Infrared optical properties of the 12 K organic superconductor  $\kappa$ -(BEDT-TTF) $_2$ Cu[N(CN) $_2$ ]Br. *Solid State Commun.* **1991**, *79*, 583–589.

55. Sasaki, T.; Ito, I.; Yoneyama, N.; Kobayashi, N.; Hanasaki, N.; Tajima, H.; Ito, T.; Iwasa, Y. Electronic correlation in the infrared optical properties of the quasi-two-dimensional  $\kappa$ -type BEDT-TTF dimer system. *Phys. Rev. B* **2004**, *69*, doi:10.1103/PhysRevB.69.064508.
56. Faltermeier, D.; Barz, J.; Dumm, M.; Dressel, M.; Drichko, N.; Petrov, B.; Semkin, V.; Vlasova, R.; Mezière, C.; Batail, P. Bandwidth-controlled Mott transition in  $\kappa$ -(BEDT-TTF)<sub>2</sub>Cu[N(CN)<sub>2</sub>]Br<sub>x</sub>Cl<sub>1-x</sub>: Optical studies of localized charge excitations. *Phys. Rev. B* **2007**, *76*, doi:10.1103/PhysRevB.76.165113.
57. Dressel, M.; Grüner, G. *Electrodynamics of Solids*; Cambridge University Press: Cambridge, UK, 2002.
58. Sasaki, T.; Yoneyama, N.; Kobayashi, N.; Ikemoto, Y.; Kimura, H. Imaging phase separation near the Mott boundary of the correlated organic superconductors  $\kappa$ -(BEDT-TTF)<sub>2</sub>X. *Phys. Rev. Lett.* **2004**, *92*, doi:10.1103/PhysRevLett.92.227001.
59. Sasaki, T.; Yoneyama, N.; Suzuki, A.; Kobayashi, N.; Ikemoto, Y.; Kimura, H. Real space imaging of the metal–insulator phase separation in the band width controlled organic mott system  $\kappa$ -(BEDT-TTF)<sub>2</sub>Cu[N(CN)<sub>2</sub>]Br. *J. Phys. Soc. Jpn.* **2005**, *74*, doi:10.1143/JPSJ.74.2351.
60. Shoenberg, D. *Magnetic Oscillation in Metals*; Cambridge University Press: Cambridge, UK, 1984.
61. Anderson, P.W. Theory of dirty superconductors. *J. Phys. Chem. Solids* **1959**, *11*, 26–30.
62. Maple, M.B. Superconductivity: A probe of the magnetic state of local moments in metals. *Appl. Phys.* **1976**, *9*, 179–204.
63. Millis, A.J.; Sachdev, S.; Varma, C.M. Inelastic scattering and pair breaking in anisotropic and isotropic superconductors. *Phys. Rev. B* **1988**, *37*, 4975–4986.
64. Radtke, R.J.; Levin, K.; Schüttler, H.-B.; Norman, N.R. Predictions for impurity-induced  $T_c$  suppression in the high-temperature superconductors. *Phys. Rev. B* **1993**, *48*, 653–656.
65. Abrikosov, A.A.; Gor'kov, L.P. Contribution to the theory of superconducting alloys with paramagnetic impurities. *Zh. Eksp. Teoret. Fiz.* **1960**, *39*, 1781–1796 [*Sov. Phys. JETP* **1961**, *12*, 1243–1253].
66. Powell, J.B.; McKenzie, R.H. Dependence of the superconducting transition temperature of organic molecular crystals on intrinsically nonmagnetic disorder: A signature of either unconventional superconductivity or the atypical formation of magnetic moments. *Phys. Rev. B* **2004**, *69*, 024519:9–024519:17.
67. Izawa, K.; Yamaguchi, H.; Sasaki, T.; Matsuda, Y. Superconducting gap structure of  $\kappa$ -(BEDT-TTF)<sub>2</sub>Cu(NCS)<sub>2</sub> probed by thermal conductivity tensor. *Phys. Rev. Lett.* **2002**, *88*, doi:10.1103/PhysRevLett.88.027002.
68. Radonjić, M.M.; Tanasković, D.; Dobrosavljević, V.; Haule, K. Influence of disorder on incoherent transport near the Mott transition. *Phys. Rev. B* **2010**, *81*, doi:10.1103/PhysRevB.81.075118.
69. Massey, J.G.; Lee, M. Direct observation of the coulomb correlation gap in a nonmetallic semiconductor, Si:B. *Phys. Rev. Lett.* **1995**, *75*, 4266–4269.